Eur. Phys. J. C 8, 573–584 (1999)
DOI 10.1007/s100529900020

THE EUROPEAN PHYSICAL JOURNAL C

Measurement of the semileptonic branching ratio of charm hadrons produced in $Z^0 \to c\bar{c}$ decays

The OPAL Collaboration

G. Abbiendi[2], K. Ackerstaff[8], G. Alexander[23], J. Allison[16], N. Altekamp[5], K.J. Anderson[9], S. Anderson[12], S. Arcelli[17], S. Asai[24], S.F. Ashby[1], D. Axen[29], G. Azuelos[18,a], A.H. Ball[17], E. Barberio[8], R.J. Barlow[16], R. Bartoldus[3], J.R. Batley[5], S. Baumann[3], J. Bechtluft[14], T. Behnke[27], K.W. Bell[20], G. Bella[23], A. Bellerive[9], S. Bentvelsen[8], S. Bethke[14], S. Betts[15], O. Biebel[14], A. Biguzzi[5], S.D. Bird[16], V. Blobel[27], I.J. Bloodworth[1], M. Bobinski[10], P. Bock[11], J. Böhme[14], D. Bonacorsi[2], M. Boutemeur[34], S. Braibant[8], P. Bright-Thomas[1], L. Brigliadori[2], R.M. Brown[20], H.J. Burckhart[8], C. Burgard[8], R. Bürgin[10], P. Capiluppi[2], R.K. Carnegie[6], A.A. Carter[13], J.R. Carter[5], C.Y. Chang[17], D.G. Charlton[1,b], D. Chrisman[4], C. Ciocca[2], P.E.L. Clarke[15], E. Clay[15], I. Cohen[23], J.E. Conboy[15], O.C. Cooke[8], C. Couyoumtzelis[13], R.L. Coxe[9], M. Cuffiani[2], S. Dado[22], G.M. Dallavalle[2], R. Davis[30], S. De Jong[12], L.A. del Pozo[4], A. de Roeck[8], K. Desch[8], B. Dienes[33,d], M.S. Dixit[7], J. Dubbert[34], E. Duchovni[26], G. Duckeck[34], I.P. Duerdoth[16], D. Eatough[16], P.G. Estabrooks[6], E. Etzion[23], H.G. Evans[9], F. Fabbri[2], M. Fanti[2], A.A. Faust[30], F. Fiedler[27], M. Fierro[2], I. Fleck[8], R. Folman[26], A. Fürtjes[8], D.I. Futyan[16], P. Gagnon[7], J.W. Gary[4], J. Gascon[18], S.M. Gascon-Shotkin[17], G. Gaycken[27], C. Geich-Gimbel[3], G. Giacomelli[2], P. Giacomelli[2], V. Gibson[5], W.R. Gibson[13], D.M. Gingrich[30,a], D. Glenzinski[9], J. Goldberg[22], W. Gorn[4], C. Grandi[2], E. Gross[26], J. Grunhaus[23], M. Gruwé[27], G.G. Hanson[12], M. Hansroul[8], M. Hapke[13], K. Harder[27], C.K. Hargrove[7], C. Hartmann[3], M. Hauschild[8], C.M. Hawkes[5], R. Hawkings[27], R.J. Hemingway[6], M. Herndon[17], G. Herten[10], R.D. Heuer[8], M.D. Hildreth[8], J.C. Hill[5], S.J. Hillier[1], P.R. Hobson[25], A. Hocker[9], R.J. Homer[1], A.K. Honma[28,a], D. Horváth[32,c], K.R. Hossain[30], R. Howard[29], P. Hüntemeyer[27], P. Igo-Kemenes[11], D.C. Imrie[25], K. Ishii[24], F.R. Jacob[20], A. Jawahery[17], H. Jeremie[18], M. Jimack[1], C.R. Jones[5], P. Jovanovic[1], T.R. Junk[6], D. Karlen[6], V. Kartvelishvili[16], K. Kawagoe[24], T. Kawamoto[24], P.I. Kayal[30], R.K. Keeler[28], R.G. Kellogg[17], B.W. Kennedy[20], A. Klier[26], S. Kluth[8], T. Kobayashi[24], M. Kobel[3,e], D.S. Koetke[6], T.P. Kokott[3], M. Kolrep[10], S. Komamiya[24], R.V. Kowalewski[28], T. Kress[11], P. Krieger[6], J. von Krogh[11], T. Kuhl[3], P. Kyberd[13], G.D. Lafferty[16], D. Lanske[14], J. Lauber[15], S.R. Lautenschlager[31], I. Lawson[28], J.G. Layter[4], D. Lazic[22], A.M. Lee[31], D. Lellouch[26], J. Letts[12], L. Levinson[26], R. Liebisch[11], B. List[8], C. Littlewood[5], A.W. Lloyd[1], S.L. Lloyd[13], F.K. Loebinger[16], G.D. Long[28], M.J. Losty[7], J. Ludwig[10], D. Liu[12], A. Macchiolo[2], A. Macpherson[30], W. Mader[3], M. Mannelli[8], S. Marcellini[2], C. Markopoulos[13], A.J. Martin[13], J.P. Martin[18], G. Martinez[17], T. Mashimo[24], P. Mättig[26], W.J. McDonald[30], J. McKenna[29], E.A. Mckigney[15], T.J. McMahon[1], R.A. McPherson[28], F. Meijers[8], S. Menke[3], F.S. Merritt[9], H. Mes[7], J. Meyer[27], A. Michelini[2], S. Mihara[24], G. Mikenberg[26], D.J. Miller[15], R. Mir[26], W. Mohr[10], A. Montanari[2], T. Mori[24], K. Nagai[8], I. Nakamura[24], H.A. Neal[12], B. Nellen[3], R. Nisius[8], S.W. O'Neale[1], F.G. Oakham[7], F. Odorici[2], H.O. Ogren[12], M.J. Oreglia[9], S. Orito[24], J. Pálinkás[33,d], G. Pásztor[32], J.R. Pater[16], G.N. Patrick[20], J. Patt[10], R. Perez-Ochoa[8], S. Petzold[27], P. Pfeifenschneider[14], J.E. Pilcher[9], J. Pinfold[30], D.E. Plane[8], P. Poffenberger[28], J. Polok[8], M. Przybycień[8], C. Rembser[8], H. Rick[8], S. Robertson[28], S.A. Robins[22], N. Rodning[30], J.M. Roney[28], K. Roscoe[16], A.M. Rossi[2], Y. Rozen[22], K. Runge[10], O. Runolfsson[8], D.R. Rust[12], K. Sachs[10], T. Saeki[24], O. Sahr[34], W.M. Sang[25], E.K.G. Sarkisyan[23], C. Sbarra[29], A.D. Schaile[34], O. Schaile[34], F. Scharf[3], P. Scharff-Hansen[8], J. Schieck[11], B. Schmitt[8], S. Schmitt[11], A. Schöning[8], M. Schröder[8], M. Schumacher[3], C. Schwick[8], W.G. Scott[20], R. Seuster[14], T.G. Shears[8], B.C. Shen[4], C.H. Shepherd-Themistocleous[8], P. Sherwood[15], G.P. Siroli[2], A. Sittler[27], A. Skuja[17], A.M. Smith[8], G.A. Snow[17], R. Sobie[28], S. Söldner-Rembold[10], M. Sproston[20], A. Stahl[3], K. Stephens[16], J. Steuerer[27], K. Stoll[10], D. Strom[19], R. Ströhmer[34], B. Surrow[8], S.D. Talbot[1], S. Tanaka[24], P. Taras[18], S. Tarem[22], R. Teuscher[8], M. Thiergen[10], M.A. Thomson[8], E. von Törne[3], E. Torrence[8], S. Towers[6], I. Trigger[18], Z. Trócsányi[33], E. Tsur[23], A.S. Turcot[9], M.F. Turner-Watson[8], R. Van Kooten[12], P. Vannerem[10], M. Verzocchi[10], H. Voss[3], F. Wäckerle[10], A. Wagner[27], C.P. Ward[5], D.R. Ward[5], P.M. Watkins[1], A.T. Watson[1], N.K. Watson[1], P.S. Wells[8], N. Wermes[3], J.S. White[6], G.W. Wilson[16], J.A. Wilson[1], T.R. Wyatt[16], S. Yamashita[24], G. Yekutieli[26], V. Zacek[18], D. Zer-Zion[8]

[1]School of Physics and Astronomy, University of Birmingham, Birmingham B15 2TT, UK
[2]Dipartimento di Fisica dell' Università di Bologna and INFN, I-40126 Bologna, Italy
[3]Physikalisches Institut, Universität Bonn, D-53115 Bonn, Germany
[4]Department of Physics, University of California, Riverside CA 92521, USA
[5]Cavendish Laboratory, Cambridge CB3 0HE, UK
[6]Ottawa-Carleton Institute for Physics, Department of Physics, Carleton University, Ottawa, Ontario K1S 5B6, Canada

[7]Centre for Research in Particle Physics, Carleton University, Ottawa, Ontario K1S 5B6, Canada
[8]CERN, European Organisation for Particle Physics, CH-1211 Geneva 23, Switzerland
[9]Enrico Fermi Institute and Department of Physics, University of Chicago, Chicago IL 60637, USA
[10]Fakultät für Physik, Albert Ludwigs Universität, D-79104 Freiburg, Germany
[11]Physikalisches Institut, Universität Heidelberg, D-69120 Heidelberg, Germany
[12]Indiana University, Department of Physics, Swain Hall West 117, Bloomington IN 47405, USA
[13]Queen Mary and Westfield College, University of London, London E1 4NS, UK
[14]Technische Hochschule Aachen, III Physikalisches Institut, Sommerfeldstrasse 26-28, D-52056 Aachen, Germany
[15]University College London, London WC1E 6BT, UK
[16]Department of Physics, Schuster Laboratory, The University, Manchester M13 9PL, UK
[17]Department of Physics, University of Maryland, College Park, MD 20742, USA
[18]Laboratoire de Physique Nucléaire, Université de Montréal, Montréal, Quebec H3C 3J7, Canada
[19]University of Oregon, Department of Physics, Eugene OR 97403, USA
[20]CLRC Rutherford Appleton Laboratory, Chilton, Didcot, Oxfordshire OX11 0QX, UK
[22]Department of Physics, Technion-Israel Institute of Technology, Haifa 32000, Israel
[23]Department of Physics and Astronomy, Tel Aviv University, Tel Aviv 69978, Israel
[24]International Centre for Elementary Particle Physics and Department of Physics, University of Tokyo, Tokyo 113, and Kobe University, Kobe 657, Japan
[25]Institute of Physical and Environmental Sciences, Brunel University, Uxbridge, Middlesex UB8 3PH, UK
[26]Particle Physics Department, Weizmann Institute of Science, Rehovot 76100, Israel
[27]Universität Hamburg/DESY, II Institut für Experimental Physik, Notkestrasse 85, D-22607 Hamburg, Germany
[28]University of Victoria, Department of Physics, P O Box 3055, Victoria BC V8W 3P6, Canada
[29]University of British Columbia, Department of Physics, Vancouver BC V6T 1Z1, Canada
[30]University of Alberta, Department of Physics, Edmonton AB T6G 2J1, Canada
[31]Duke University, Dept of Physics, Durham, NC 27708-0305, USA
[32]Research Institute for Particle and Nuclear Physics, H-1525 Budapest, P O Box 49, Hungary
[33]Institute of Nuclear Research, H-4001 Debrecen, P O Box 51, Hungary
[34]Ludwigs-Maximilians-Universität München, Sektion Physik, Am Coulombwall 1, D-85748 Garching, Germany

Recveived: 17 September 1998 / Published online: 1 March 1999

Abstract. The inclusive charm hadron semileptonic branching fractions $B(c \to e)$ and $B(c \to \mu)$ in $Z^0 \to c\bar{c}$ events have been determined using 4.4 million hadronic Z^0 decays collected with the OPAL detector at LEP. A charm-enriched sample is obtained by selecting events with reconstructed $D^{*\pm}$ mesons. Using leptons found in the hemisphere opposite that of the $D^{*\pm}$ mesons, the semileptonic branching fractions of charm hadrons are measured to be

$$B(c \to e) = 0.103 \pm 0.009^{+0.009}_{-0.008} \quad \text{and} \quad B(c \to \mu) = 0.090 \pm 0.007^{+0.007}_{-0.006},$$

where the first errors are in each case statistical and the second systematic. Combining these measurements, an inclusive semileptonic branching fraction of charm hadrons of

$$B(c \to \ell) = 0.095 \pm 0.006^{+0.007}_{-0.006}$$

is obtained.

1 Introduction

The inclusive charm hadron semileptonic branching fractions $B(c \to e)$ and $B(c \to \mu)$ are defined as the average of the semileptonic branching ratios of weakly decaying charm hadrons weighted by their production rates in prompt charm events, $Z^0 \to c\bar{c}$. Inclusive semileptonic branching ratios are a means to investigate the dynamics of heavy quark decays, and have been studied in much detail for bottom quarks [1]. The inclusive semileptonic branching ratio of charm hadrons has not previously been measured at LEP, even though it is an important input to a number of measurements performed at energies around the Z^0 resonance [2].

The inclusive semileptonic branching fraction of charm hadrons has so far been measured at centre-of-mass energies significantly below the Z^0 mass [3,4]. Many of these measurements depend strongly on the modelling of the $b \to \ell$ background in the sample. In this paper a measurement of $B(c \to e)$ and $B(c \to \mu)$ is presented which is much less dependent on the bottom background, since it is done in a sample of events enriched in $Z^0 \to c\bar{c}$ decays. This sample is prepared by selecting highly energetic D^{*+}

[a] and at TRIUMF, Vancouver, Canada V6T 2A3
[b] and Royal Society University Research Fellow
[c] and Institute of Nuclear Research, Debrecen, Hungary
[d] and Department of Experimental Physics, Lajos Kossuth University, Debrecen, Hungary
[e] on leave of absence from the University of Freiburg

mesons[1]. The hemisphere opposite to the one containing the D^{*+} meson is searched for a lepton, yielding a measurement of the inclusive semileptonic branching fraction of charm hadrons.

The paper is organised as follows. The principle of the analysis, in particular the method used to subtract the background, is discussed in Sect. 2. After a brief review of the event selection in Sect. 3, the identification of charm events using reconstructed D^{*+} mesons is described and the determination of the charm fraction in the sample is summarised in Sect. 4. The preparation of the lepton sample in charm-tagged events and the measurement of the background in this sample is described in Sect. 5, followed by the presentation of the results in Sect. 6. Systematic errors are given in Sect. 7.

2 Analysis principle

A sample of $Z^0 \to c\bar{c}$ enriched events is found using reconstructed D^{*+} mesons. Each event is divided into two hemispheres by the plane perpendicular to the thrust axis. Leptons are searched for in the hemisphere opposite the D^{*+} meson. Background is suppressed by requiring that the D^* and the ℓ have opposite charge. The number of leptons found in the hemisphere opposite that of the D^* meson has contributions from prompt charm decays, $c \to \ell$, from prompt bottom decays, $b \to \ell$, from cascade decays, $b \to c \to \ell$, and from background. It can be written as

$$\begin{aligned} N^{\mathrm{cand}}_{\mathrm{D}^{*+},\ell^-} = N^{\mathrm{sig}}_{\mathrm{D}^{*+}} \cdot \Big\{ & f_{\mathrm{c}}^{\mathrm{D}^{*+}} \mathrm{B}(\mathrm{c} \to \ell) \epsilon_\ell^{\mathrm{c}\to\ell} \\ & + (1 - f_{\mathrm{c}}^{\mathrm{D}^{*+}}) \Big[\chi_{eff} \mathrm{B}(\mathrm{b} \to \ell) \epsilon_\ell^{\mathrm{b}\to\ell} \\ & + (1 - \chi_{\mathrm{eff}}) \mathrm{B}(\mathrm{b} \to \mathrm{c} \to \ell) \epsilon_\ell^{\mathrm{b}\to\mathrm{c}\to\ell} \Big] \Big\} + N^{+-}_{\mathrm{bgd}} \,. \end{aligned} \quad (1)$$

Here $N^{\mathrm{sig}}_{\mathrm{D}^{*+}}$ is the number of D^{*+} mesons found in the data sample, $f_{\mathrm{c}}^{\mathrm{D}^{*+}}$ is the fraction of these D^{*+} mesons coming from $Z^0 \to c\bar{c}$ events, and N^{+-}_{bgd} is the number of background events, where either a D^{*+}, a lepton or both are misidentified, but where the charge correlation is correct between the two hemispheres. This background will be denoted as "combinatorial background". The parameter χ_{eff} is the effective mixing parameter for the mixture of neutral B mesons selected, and $\epsilon_\ell^{\mathrm{c}\to\ell}$, $\epsilon_\ell^{\mathrm{b}\to\ell}$ and $\epsilon_\ell^{\mathrm{b}\to\mathrm{c}\to\ell}$ are the efficiencies to find a lepton opposite a D^{*+} in the channel indicated, with the correct charge correlation. To simplify this and the following equations, leptons produced in $b \to \bar{c} \to \ell$ decays and $b \to \tau \to \ell$ decays are included in the $b \to \ell$ decays. Since a pair of leptons, one with the correct and one with the wrong charge correlation, is produced in $b \to J/\Psi \to \ell^+\ell^-$ decays they are equally split between the $b \to \ell$ and the $b \to c \to \ell$ decays.

The goal of this analysis is the measurement of $B(c \to \ell)$. It is extracted from $N^{\mathrm{c}}_{\mathrm{D}^{*+},\ell^-}$, the number of $Z^0 \to c\bar{c}$ events where simultaneously a D^{*+} meson in one hemisphere and a lepton in the opposite hemisphere is found:

$$N^{\mathrm{c}}_{\mathrm{D}^{*+},\ell^-} = N^{\mathrm{sig}}_{\mathrm{D}^{*+}} \, f_{\mathrm{c}}^{\mathrm{D}^{*+}} \, \mathrm{B}(\mathrm{c} \to \ell) \, \epsilon_\ell^{\mathrm{c}\to\ell} \,. \quad (2)$$

A sample of events which does not contain contributions from prompt charm decays is prepared by selecting events where the D^{*+} and the lepton have equal charge:

$$\begin{aligned} N^{\mathrm{cand}}_{\mathrm{D}^{*+},\ell^+} = N^{\mathrm{sig}}_{\mathrm{D}^{*+}} (1 - f_{\mathrm{c}}^{\mathrm{D}^{*+}}) \big\{ & (1 - \chi_{eff}) \mathrm{B}(\mathrm{b} \to \ell) \epsilon_\ell^{\mathrm{b}\to\ell} \\ & + \chi_{\mathrm{eff}} \mathrm{B}(\mathrm{b} \to \mathrm{c} \to \ell) \epsilon_\ell^{\mathrm{b}\to\mathrm{c}\to\ell} \big\} + N^{++}_{\mathrm{bgd}} \,. \end{aligned} \quad (3)$$

Here N^{++}_{bgd} is the number of combinatorial background events in this wrong sign sample. The number of leptons from charm hadron decays can be calculated by solving the two equations 1 and 3 for $N^{\mathrm{c}}_{\mathrm{D}^{*+},\ell^-}$ defined in equation 2. The solution can be written in terms of the difference of the two samples of events and two small corrections,

$$N^{\mathrm{c}}_{\mathrm{D}^{*+},\ell^-} = (N^{\mathrm{cand}}_{\mathrm{D}^{*+},\ell^-} - N^{\mathrm{cand}}_{\mathrm{D}^{*+},\ell^+}) - \Delta N_{\mathrm{b}} - \Delta N_{\mathrm{bgd}} \,. \quad (4)$$

The first correction, ΔN_{b}, can be derived directly from equation 1 and equation 3 and reflects the fact that mixing affects both samples differently. It is calculable from the known branching ratios and the mixing parameter:

$$\begin{aligned} \Delta N_{\mathrm{b}} = & N^{\mathrm{sig}}_{\mathrm{D}^{*+}} (1 - f_{\mathrm{c}}^{\mathrm{D}^{*+}}) (1 - 2\chi_{\mathrm{eff}}) \\ & \times \big\{ \mathrm{B}(\mathrm{b} \to \mathrm{c} \to \ell) \epsilon_\ell^{\mathrm{b}\to\mathrm{c}\to\ell} - \mathrm{B}(\mathrm{b} \to \ell) \epsilon_\ell^{\mathrm{b}\to\ell} \big\} \,. \end{aligned} \quad (5)$$

The second correction, ΔN_{bgd}, is the difference between the combinatorial background term in both samples, $\Delta N_{\mathrm{bgd}} = N^{+-}_{\mathrm{bgd}} - N^{++}_{\mathrm{bgd}}$. This number is determined using both data and Monte Carlo simulations, as will be discussed in Sect. 5.1. Finally the inclusive semileptonic branching ratio of charm hadrons, $B(c \to \ell)$, is calculated from equation 2 as

$$\mathrm{B}(\mathrm{c} \to \ell) = N^{\mathrm{c}}_{\mathrm{D}^{*+},\ell^-} \frac{1}{N^{\mathrm{sig}}_{\mathrm{D}^{*+}} f_{\mathrm{c}}^{\mathrm{D}^{*+}} \epsilon_\ell^{\mathrm{c}\to\ell}} \,, \quad (6)$$

where the number of events with a D^{*+} meson, the number of leptons found in this sample, the efficiencies to reconstruct the leptons in the tagged charm sample, and ΔN_{b} and ΔN_{bgd} have to be known. Each of these inputs will be discussed in the following sections.

3 The OPAL detector and event selection

A detailed description of the OPAL detector can be found elsewhere [5]. The most relevant parts of the detector for this analysis are the tracking chambers, the electromagnetic calorimeter, and the muon chambers. The central detector provides precise measurements of the momenta of charged particles by the curvature of their trajectories in a solenoidal magnetic field of 0.435 T. The electromagnetic calorimeter consists of approximately 12000 lead glass blocks, which completely cover the azimuthal range

[1] Throughout this note charge conjugation is always implied, unless explicitly stated otherwise.

up to polar angles[2] of $|\cos\theta| < 0.98$. Nearly the entire detector is surrounded with at least three layers of muon chambers, which are placed behind an approximately one meter thick iron magnet flux return yoke.

Hadronic Z^0 decays are selected using the number of reconstructed charged tracks and the energy deposited in the calorimeter, as described in [6]. The analysis uses an initial sample of 4.4 million hadronic decays of the Z^0 collected between 1990 and 1995.

Hadronic decays of the Z^0 have been simulated using the JETSET 7.4 Monte Carlo model [7] with parameters tuned to the data [8]. The Monte Carlo samples are about five times larger than the collected data sample. Heavy quark fragmentation has been implemented using the model of Peterson et al. [9] with fragmentation parameters determined from LEP data [10]. The samples have been passed through a detailed simulation of the OPAL detector [11] before being analysed using the same programs as for the data. Jets are reconstructed in the events by the JADE jet finder using the E0 scheme with a cut-off parameter $x_{min} = 49\ \mathrm{GeV}^2$ [12].

4 Charm tagging

The tagging of $Z^0 \to c\bar{c}$ events is based on the reconstruction of charged D^{*+} mesons in five different decay channels. The identification algorithm and the method to separate the different sources contributing to the observed D^{*+} signal have been presented in a previous OPAL paper [13], and will only be briefly reviewed.

The D^{*+} mesons are reconstructed in the following five decay channels:

$$
\begin{aligned}
&D^{*+} \to D^0\pi^+ \\
&\qquad \hookrightarrow\ K^-\pi^+, && \text{“3-prong”} \\
&\qquad \hookrightarrow\ K^-e^+\nu_e, && \text{“electron”} \\
&\qquad \hookrightarrow\ K^-\mu^+\nu_\mu, && \text{“muon”} \\
&\qquad \hookrightarrow\ K^-\pi^+\pi^0, && \text{“satellite”} \\
&\qquad \hookrightarrow\ K^-\pi^+\pi^-\pi^+, && \text{“5-prong”}\ .
\end{aligned}
$$

The muon and the electron channels are collectively referred to as “semileptonic”. No attempt is made to reconstruct the π^0 in the satellite channel, nor the neutrino in the two semileptonic channels. Electrons are identified based on their specific energy loss, $\mathrm{d}E/\mathrm{d}x$, in the central tracking chamber and the energy deposition in the electromagnetic calorimeter. An artificial neural network trained on simulated events is used to perform the selection [14]. Electrons from photon conversions are rejected as in [15]. Muons are selected using matching of track segments of the central tracking chambers and the muon chambers, as described in [15]. The purity of kaons is enhanced by requiring that the $\mathrm{d}E/\mathrm{d}x$ measurement of the candidate is compatible with that expected for a kaon. If the track combination has an invariant mass M_{D^0} within the limits given in Table 1, the combination is accepted as a D^0 candidate. The combinatorial background is reduced by a cut on the cosine of the helicity angle, $\cos\theta^*$, measured between the direction of the D^0 in the laboratory frame and the direction of the kaon in the rest-frame of the D^0 candidate. Background is expected to peak at ± 1 in this variable, while true D^0 mesons are uniformly distributed. These D^0 candidates are combined with a candidate for the pion in the $D^{*+} \to D^0\pi^+$ decay. Background from bottom decays and combinatorial background is reduced by selecting candidates with a large scaled energy, $x_{D^{*+}} = E^{\mathrm{cand}}_{D^{*+}}/E_{\mathrm{beam}}$. The final selection is made on the mass difference $\Delta M = M_{D^{*+}} - M_{D^0}$ between the D^{*+} candidate and the corresponding D^0 candidate.

If more than one D^{*+} candidate is found in an event, only one candidate is accepted according to the following procedure. A 3-prong decay is preferred over a semileptonic one, which in turn is preferred over a satellite, and a 5-prong decay is selected last. If more than one candidate is found within the same decay channel, the one with M_{D^0} closest to its nominal value of 1.864 GeV [1] (1.6 GeV for the satellite) is selected. In Fig. 1, the mass difference distributions $\Delta M = M_{D^{*+}} - M_{D^0}$ are shown for the different channels. In total 27662 candidates are selected in all five channels.

The selected sample of D^{*+} candidates has contributions from: D^{*+} mesons produced in $Z^0 \to c\bar{c}$ events (signal); D^{*+} mesons produced in $Z^0 \to b\bar{b}$ events; D^{*+} mesons produced in events where a $c\bar{c}$ pair is produced in the splitting of a gluon; combinatorial background. The combinatorial background in the sample of D^{*+} mesons is subtracted on a statistical basis using an independent sample of background candidate events, selected based on a hemisphere mixing technique first introduced in [16]. The candidate for the pion in the $D^{*+} \to D^0\pi^+$ decay is selected in the hemisphere opposite to the rest of the candidate, and reflected through the origin. This sample of candidates has been shown to be an unbiased estimator of the combinatorial background [16,17] and to reliably model the shape of the background. The contribution from gluon splitting is estimated and subtracted from the sample based on the OPAL measurement of the multiplicity of such events in hadronic Z^0 decays [18]. For the cuts used in this analysis, $g \to c\bar{c}$ events contribute $(1.1 \pm 0.4)\%$ to the signal. After all corrections, and after combinatorial background subtraction, 15784 ± 99 D^{*+} mesons are used in the subsequent analysis. The error quoted is the statistical uncertainty of the combinatorial background subtraction [3].

The remaining two sources of D^{*+} production, $Z^0 \to c\bar{c} \to D^{*+}X$ and $Z^0 \to b\bar{b} \to D^{*+}X$, are separated by

[2] The OPAL coordinate system is defined as a Cartesian coordinate system, with the x-axis pointing horizontally towards the centre of the LEP ring, the z-axis in the direction of the outgoing electrons, and the y-axis points approximately vertically upwards. The polar angle is measured with respect to the z-axis.

[3] The error quoted here is smaller than the expected statistical error from the sample size since the sample used to determine the background is larger than the actual background. The error quoted contains a contribution from the sample size and an additional error from the normalisation of the background in the sidebands.

Table 1. List of selection cuts used in the D^{*+} reconstructions. $W^{KK}_{dE/dx}$ is the probability that the measured dE/dx value is compatible with that expected for a kaon at the measured momentum. This cut is only applied to the kaon candidate in the D^0 decay. The background distribution thus obtained is normalised to the candidate ΔM distribution in the range 0.18 GeV $< \Delta M <$ 0.20 GeV (0.19 GeV $< \Delta M <$ 0.22 GeV in the semileptonic channels). In the last two lines of the table, the relative abundance of each channel and the signal/background ratio is given, as measured from the data

		D^0 decay mode			
Variable		3-prong	semileptonic	satellite	5-prong
$x_{D^{*+}}$ range		0.4-1.0	0.4-1.0	0.4-1.0	0.5-1.0
M_{D^0} [GeV]		1.79-1.94	1.20-1.80	1.41-1.77	1.79-1.94
ΔM [GeV]		0.142-0.149	0.140-0.162	0.141-0.151	0.142-0.149
$\cos\theta^*$	$x_{D^{*+}} < 0.5$		-0.8-0.8		–
$\cos\theta^*$	$x_{D^{*+}} > 0.5$		-0.9-1.0		
$W^{KK}_{dE/dx}$	$x_{D^{*+}} < 0.5$		> 0.1		–
Relative abundance		0.231	0.121	0.355	0.293
Signal/background		3.496	3.233	1.223	0.879

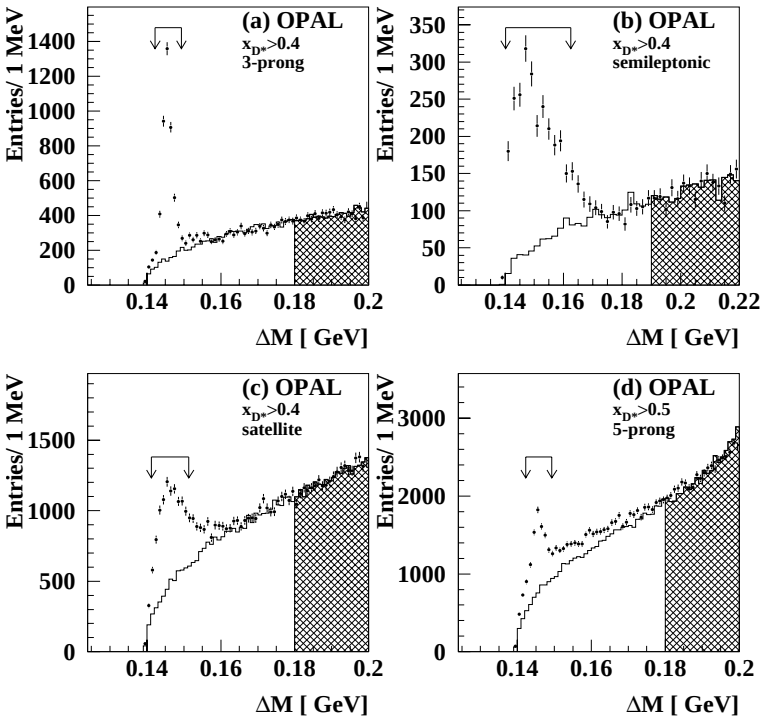

Fig. 1a–d. Distributions of the mass difference $\Delta M = M_{D^{*+}} - M_{D^0}$ reconstructed in the four different D^{*+} channels. The arrows indicate the range in ΔM considered as signal. The background estimator distributions are superimposed, normalised to the signal distribution at large values of ΔM indicated by the cross-hatched area. Note that the significant tails in the ΔM distribution above the expected signal, particularly in **c** and **d**, are caused by partially reconstructed D^{*+} mesons, and is properly treated by the background estimator (see text)

applying three different flavour tagging methods, based on lifetime information, jet shapes and hemisphere charge information, as described in [13]. Combining all D^{*+} channels, the overall charm fraction is determined to be:

$$f_c^{D^{*+}} = 0.774 \pm 0.008 \pm 0.022, \quad (7)$$

where the first error is statistical and the second systematic. The dominant systematic errors are from the estimation of the background in the D^{*+} sample, and from modelling the charm physics parameters used in the flavour separation. A breakdown of the systematic error into its components which are relevant for this analysis is given in Table 2. The errors are split into two groups: one group which is uncorrelated to errors encountered when identifying leptons in this sample of events, and a second group of correlated errors. In the latter case the errors are signed indicating in which direction the result changes if the underlying physics variable is changed in the direction indicated in the table. More details of the procedure and of all systematic errors are given in [13].

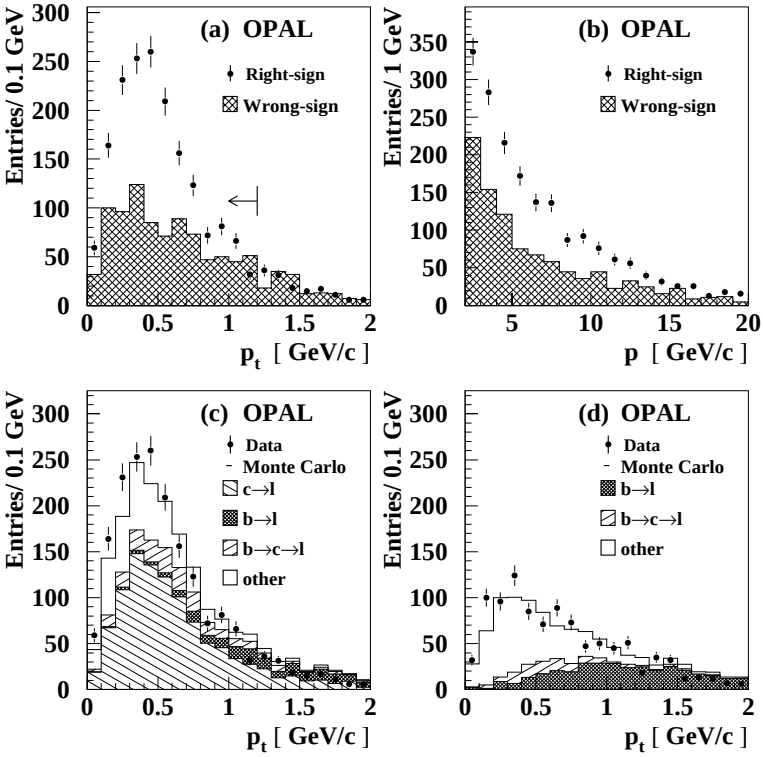

Fig. 2a–d. Transverse momentum spectrum **a** and momentum spectrum **b** of the selected lepton candidates. The arrow in **a** indicates the position of the p_t cut. The hatched distribution is the background estimated using the wrong sign event sample. Composition of the p_t spectrum in the Monte Carlo for right sign **c**, and for wrong sign events **d**

Table 2. List of the systematic errors on the charm fraction $f_c^{D^{*+}}$ in the D^{*+} sample. The top part of the table contains that part of the error which is uncorrelated with the systematic error associated to the reconstruction of leptons in the D^{*+} sample. The signs given for the errors in the lower part indicate the direction in which the result changes for a change of the relevant variable by the amount and direction indicated in the middle column

Error source	Variation	Error
Total uncorrelated		±0.021
B mixing	$\chi_{\text{eff}} : +11\%$	−0.002
Fragmentation modelling	$\langle x_E \rangle_B : +0.008,$	
	$\langle x_E \rangle_D : +0.009$	+0.004
Gluon splitting	$\bar{n}_{g\to c\bar{c}} : +21\%$	−0.002
Total		± 0.022

5 The $D^{*+}\ell^-$ sample

The $D^{*+}\ell^-$ sample is found by searching the hemisphere opposite the identified D^{*+} meson for a lepton with a charge opposite to that of the D^{*+} candidate. Electrons are identified using a neural network technique [14]. The network used in this part of the analysis is slightly simplified compared to the one used in [14], using only 6 inputs, 8 nodes in one hidden layer, and one output. The input variables are

- the difference between the measured specific energy loss, dE/dx, and that expected for an electron, divided by its expected uncertainty;
- the experimental uncertainty on dE/dx;
- E/p, the energy of the electromagnetic cluster associated with the track inside a cone with a half opening angle of 30 mrad, divided by the measured track momentum;
- the number of electromagnetic blocks in the cluster;
- the momentum of the track;
- the polar angle, $|\cos\theta|$, of the track.

All variables are well modelled in the Monte Carlo simulation, thus ensuring a reliable calculation of the selection efficiency.

Muons are identified based on the χ^2 of the matching between track segments in the central tracking chambers and in the muon chambers [15]. In addition the specific energy loss, dE/dx, has to be compatible with that expected for a muon at the measured momentum.

To reduce systematic uncertainties, electrons are reconstructed only in the central part of the OPAL detector, $|\cos\theta| < 0.715$, while muons are required to satisfy $|\cos\theta| < 0.9$. To increase the purity of the electron and muon samples, candidate tracks must have momenta greater than 2 GeV/c. Events from bottom decays are suppressed by selecting only candidates with $p_t < 1.2$ GeV/c for both electrons and muons, where the transverse momentum, p_t, is measured with respect to the axis of the jet containing the lepton candidate, including the lepton candidate itself in the jet-axis calculation. After all cuts, a total of 661 electron and 1045 muon candidates are selected.

The efficiency to select a lepton is calculated using Monte Carlo simulations. It is calculated from events where a D^{*+} meson is reconstructed in one hemisphere, and a

Table 3. Efficiencies to reconstruct an electron or a muon opposite a D^{*+} meson separately for the different sources after applying all cuts. The errors quoted are purely statistical

	Efficiencies for	
Source	Electrons	Muons
$c \to \ell$	0.302 ± 0.007	0.433 ± 0.008
$b \to \ell$	0.305 ± 0.015	0.305 ± 0.015
$b \to c \to \ell$	0.222 ± 0.013	0.346 ± 0.015
$b \to \bar{c} \to \ell$	0.213 ± 0.031	0.315 ± 0.036

Table 4. Semileptonic branching ratios as given in [1] and [10]

Source	Branching ratio	ref.
$b \to \ell$	0.1099 ± 0.0023	[1]
$b \to c \to \ell$	0.0780 ± 0.0060	[1]
$b \to \bar{c} \to \ell$	0.0130 ± 0.0050	[10]
$b \to \tau \to \ell$	0.0045 ± 0.0007	[1]
$b \to J/\Psi \to \ell^+\ell^-$	0.0007 ± 0.0001	[1]

lepton in the other, so that possible correlations between both hemispheres are taken into account. The $\epsilon_{c\to\ell}$ efficiencies are found to be

$$\epsilon_{c\to e} = 0.302 \pm 0.007 \quad \text{and} \quad \epsilon_{c\to\mu} = 0.433 \pm 0.008, \quad (8)$$

where the errors are due to the finite Monte Carlo statistics. A list of all efficiencies, including those for leptons in bottom events, is given in Table 3. The overall difference in the efficiencies for muons and electrons is mostly due to the larger range of $\cos\theta$ used for the muons. The ratio $\epsilon_{b\to\ell}/\epsilon_{c\to\ell}$ is larger for electrons than it is for muons, because the electron identification algorithm depends more strongly on p_t than the muon identification does, the former being more efficient at large p_t. Since $b \to \ell$ events have on average a larger p_t, electrons are found with larger efficiency in $b \to \ell$ events. The p_t and p distributions of the selected candidates are shown in Figs. 2a and 2b, respectively. The distributions of the wrong sign candidates are superimposed.

5.1 Combinatorial background estimation

Background in the $D^{*+}\ell^-$ events is estimated from the data with the help of the wrong sign $D^{*+}\ell^+$ sample. Subtracting the number of events found in the wrong sign sample from the number of events found in the right sign sample gives an estimate of the number of $c \to \ell$ decays, with only a small contribution remaining from background events (see equation 4). The compositions of the right sign and of the wrong sign samples are shown in Figs. 2c and 2d.

The subtraction of the combinatorial background relies on the assumption that these events are equally distributed between the right and the wrong sign sample,

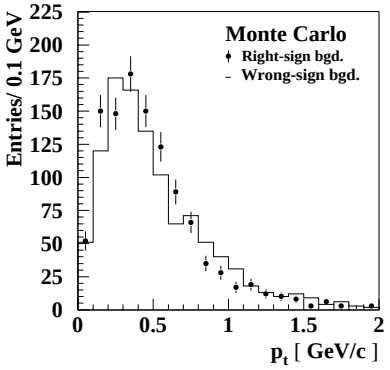

Fig. 3. Comparison of the right sign combinatorial background (points with error bars) and the wrong sign combinatorial background component (line histogram) in the simulation.

namely that $N^{+-}_{bgd} = N^{++}_{bgd}$. This subtraction procedure requires no explicit knowledge of the hadronic contamination in the lepton sample, since it is subtracted together with the wrong sign events. In Fig. 3, the shape of the p_t distribution of the combinatorial background in the right sign sample, N^{+-}_{bgd}, is compared to the combinatorial component in the wrong sign sample, N^{++}_{bgd}. Good agreement is observed for the fraction of events below the applied cut of 1.2 GeV in the right and in the wrong sign combinatorial background. The shapes are slightly different which is attributed to different contributions from bottom events to both samples. However since only the overall number of events is needed in this analysis the difference has a very small influence on the final result.

Monte Carlo studies show that the assumption $N^{+-}_{bgd} = N^{++}_{bgd}$ is not entirely correct, since a particular class of events, accounting for less than 10% of the background, is found more often in the right sign sample than in the wrong sign sample. These events consist of a partially reconstructed D^{*+} meson opposite a correctly identified lepton with the correct charge correlation. The number of such events found in the wrong sign sample amounts to only 55% of the number of the same type of events found in the right sign sample. The total number of these events in the right sign sample has been measured in [13] from data. Relative to the combinatorial background, they account for $(8.5 \pm 2.2)\%$ of the total right sign sample. The background subtracted sample is therefore corrected for the fraction of these events, namely by +45% of the $(8.5 \pm 2.2)\%$. This corresponds to a background charge asymmetry of $\Delta N_{bgd} = +(43 \pm 11)$ events, where the error is dominated by the fraction of such events measured in the data. An additional modelling error of 50% of this correction is applied, as will be discussed in Sect. 7.

5.2 Estimation of the bottom background

The sample of tagged $D^{*+}\ell^-$ events has a charm purity of about 60%. Non-leptonic background accounts for 8% of the electron candidates and 15% of the muon candidates. The rest consists of correctly identified leptons

from a number of different sources. The sample composition as determined from the Monte Carlo simulations is shown in Figs. 2c and 2d. Since the charges of the D^* and the ℓ should be opposite in the $D^{*+}\ell^-$ sample, any effect which influences the charge correlation between the two hemispheres influences the flavour composition. The most important of these is B-meson mixing. If mixing has occurred in either hemisphere, the charge correlation between the primary quark and the corresponding D^{*+} meson is changed. The total probability in b-events that mixing has changed the charge correlation is given by

$$\chi_{D^{*+}\ell^-} = \chi_{D^{*+}}(1-\chi_\ell) + \chi_\ell(1-\chi_{D^{*+}}) \,, \qquad (9)$$

where $\chi_{D^{*+}}, \chi_\ell$ are the effective mixing parameters applicable to the D^{*+} and the lepton, respectively. These effective mixing parameters depend on the fractions of B_d^0 and B_s^0 mesons in the sample under consideration, and on the mixing in the B_d^0 and the B_s^0 system. The average mixing in the B_d^0 system is measured to be $\chi_d = 0.172 \pm 0.010$ [1]. The LEP combined lower limit for B_s^0 mixing given in [1] corresponds to a lower limit on χ_s of 0.4975 at 95% confidence level. In this analysis, χ_s is varied between 0.49 and the maximum value of 0.50.

Most D^{*+} mesons in $Z^0 \to b\overline{b}$ events originate from decays of the B_d^0 meson. In [19] this fraction has been determined to be $r_d^{D^{*+}} = 0.81^{+0.05}_{-0.11}$. The fraction of D^{*+} that come from B_s^0 mesons has been estimated to be $r_s^{D^{*+}} = 0.043 \pm 0.039$ [19]. The effective mixing in the hemisphere containing the D^{*+} meson is therefore

$$\chi_{D^{*+}} = r_d^{D^{*+}} \cdot \chi_d + r_s^{D^{*+}} \cdot \chi_s = 0.161^{+0.023}_{-0.028} \,. \qquad (10)$$

The fraction of leptons produced in direct weak decays of B_d^0 and B_s^0 mesons is determined from the fractions of weakly decaying B-hadrons in $Z^0 \to b\overline{b}$ events by weighting with the lifetimes of the B-hadrons species [1]. This is done in order to correct for the different semileptonic branching ratios and leads to the values $r_d^\ell = 0.398 \pm 0.022$ and $r_s^\ell = 0.105^{+0.019}_{-0.020}$, respectively. The effective mixing parameter is

$$\chi_{\ell^-} = r_d^\ell \cdot \chi_d + r_s^\ell \cdot \chi_s = 0.120 \pm 0.011 \,. \qquad (11)$$

A significant part of the leptons in the sample is produced in cascade decays of the B meson, where the lepton is produced in the weak decay of the charmed hadron in the B decay. Since the fractions of semileptonic decays in cascade b decays from B^0 and B_s^0 mesons is not necessarily the same as in direct b decays, the effective mixing in cascade decays can be slightly different. The relative contribution of neutral B mesons is found to be $r_d^{\ell'} = 0.351 \pm 0.051$ and $r_s^{\ell'} = 0.048 \pm 0.031$ using branching ratios and production fractions from [1].

In addition, D^{*+} mesons with the wrong sign can be produced in bottom decays, where a $\overline{c}$ quark is produced in the decay of a virtual W. This can be expressed in terms of a mixing-like parameter ζ_D. As in [20], a value of $\zeta_D = 0.025 \pm 0.025$ is used. The effective mixing parameter is then

$$\chi_{\rm eff} = \chi_{D^{*+}\ell^-}(1-\zeta_D) + \zeta_D(1-\chi_{D^{*+}\ell^-}) \,, \qquad (12)$$

neglecting terms which are quadratic in either $\chi_{D^{*+}\ell^-}$ or ζ_D. The effective mixing parameter for the $D^{*+}\ell^-$ sample is finally estimated to be

$$\chi_{\rm eff} = 0.255^{+0.033}_{-0.034}. \qquad (13)$$

This value includes an uncertainty of ± 0.016 from taking the possible differences between mixing in direct and mixing in cascade b decays into account.

In total, the contribution to the background from bottom events is calculated according to equation 5, using the efficiencies listed in Table 3, the branching ratios given in Table 4, and the effective mixing parameter determined above. The total contribution amounts to $\Delta N_b = -(57 \pm 7)$ events.

Table 5. Summary of selected events in each sample, and number of events after background subtraction

Sample	D^*e	$D^*\mu$
Right-sign	661	1045
Wrong-sign	305	558
$N^c_{D^{*+},\ell^-}$	378 ± 31	476 ± 40

6 Results

The number of $D^{*+}\ell^-$ combinations in charm events is determined according to equation 4. The background subtracted momentum and transverse momentum spectra for electrons and muons are shown separately in Fig. 4. The distributions are further corrected for the effects of mixing and for the charge asymmetry in the background, as described in Sect. 5.1.

The total number of leptons from charm hadron decays is $N^c_{D^{*+},e^-} = 378 \pm 31$ and $N^c_{D^{*+},\mu^-} = 476 \pm 40$, respectively. The quoted error is purely statistical. In Table 5, a summary of the selected events in each sample is shown. Combining these measurements with the total number of selected D^{*+} mesons, $N_{D^{*+}} = 15784 \pm 99$, the appropriate charm fraction, and the lepton efficiencies, the inclusive semileptonic branching ratios of charm hadrons in $Z^0 \to c\overline{c}$ events are determined to be

$$B(c \to e) = 0.103 \pm 0.009 \quad \text{and} \quad B(c \to \mu) = 0.090 \pm 0.007 \,.$$

Here, the quoted errors are only statistical. The semileptonic branching fraction of charm hadrons derived from these individual results is

$$B(c \to \ell) = 0.095 \pm 0.006.$$

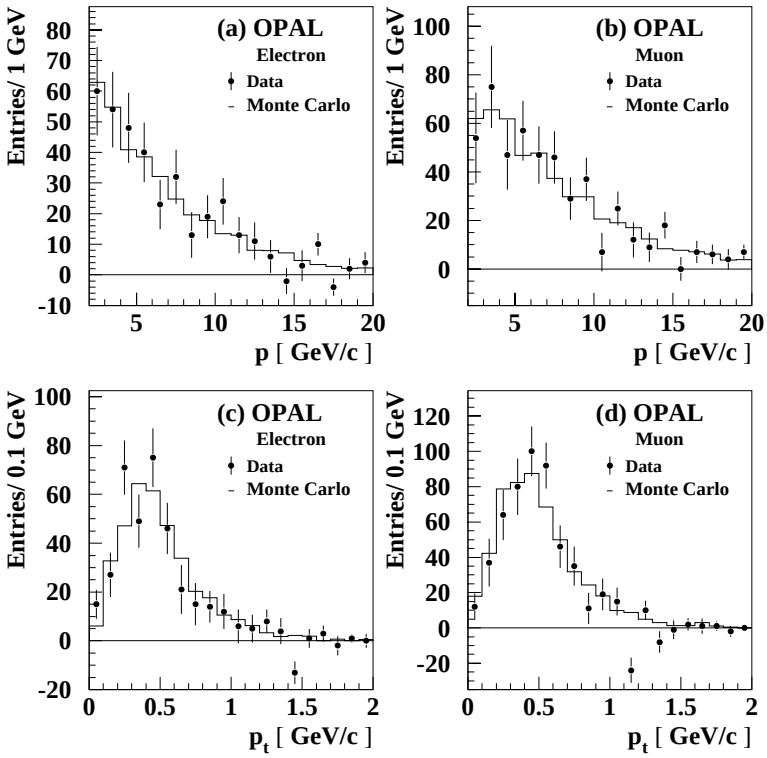

Fig. 4a–d. Momentum spectra after background subtraction for electrons **a** and muons **b**, and transverse momentum spectra for electrons **c** and muons **d**. Points are data, the line histogram is the Monte Carlo prediction. Both data and Monte Carlo include the residual background contributions from bottom events and from the background charge asymmetry

7 Systematic errors

In this section, the different sources of systematic errors are discussed. A breakdown of all errors considered is summarised in Table 6. All errors in this section are given relative to the inclusive B(c $\to \ell$) branching ratio, if not otherwise stated.

– Modelling errors

– c $\to \ell$ modelling: The momentum spectrum of leptons in c $\to \ell$ decays is described by the ACCMM model. Using the range of parameters recommended in [10] this corresponds to an error of $^{+5.6}_{-3.3}$% of the charm semileptonic branching ratio. The size of the error is largely dependent on the momentum cut used in the identification of electrons and muons. It is the dominant error in the analysis, largely caused by the comparatively poor knowledge of the modelling of the momentum spectrum of leptons in semileptonic charm decays.

– b $\to \ell$ modelling: The momentum distribution of the leptons in bottom decays influences the tagging efficiencies. Following the recommendations in [10] this has been studied by reweighting the lepton spectrum in the Monte Carlo simulation to different theoretical models, with ranges of parameters chosen such that the experimental errors are covered. The ACCMM [21] model is used to obtain the central value, and the ISGW and the ISGW** [22] models are used for the $\pm 1\sigma$ variation around the central value, and the efficiencies are recalculated. The errors found are 0.1%.

– b $\to$ c $\to \ell$ modelling: The b $\to$ c $\to \ell$ modelling error is derived following the procedure proposed in [10]. Essentially the b $\to$ D part and the c $\to \ell$ part are varied separately, using the models proposed for the relevant decay. The variation of the c $\to \ell$ part is assumed to be fully correlated to the one of the primary c $\to \ell$ decays. The lepton efficiencies are recalculated. The errors for the final result are $^{+0.2}_{-0.1}$%.

– Fragmentation modelling: The fragmentation parameters in the Monte Carlo simulation have been varied to change the mean scaled energy of weakly decaying bottom and charm hadrons around their experimental values of $\langle x_E \rangle_{\mathrm{B}} = 0.702 \pm 0.008$ and $\langle x_E \rangle_{\mathrm{D}} = 0.484 \pm 0.009$ respectively [10]. This study is done using the Peterson fragmentation model [9]. This results in an error of $\pm 0.6\%$. The error is dominated by the charm fragmentation function, with the uncertainties from varying the bottom fragmentation parameters contributing $\pm 0.15\%$. In addition, the Peterson fragmentation model has been replaced by the Collins and Spiller fragmentation model [23] and by the Kartvelishvili fragmentation model [24]. The parameters for these models have been adjusted to the same mean scaled energy as for the Peterson function. The largest deviation between the different models is used as a systematic error. It is dominated by the contribution from the charm fragmentation function, of $\pm 0.7\%$. Combined with the error using different parameters for the Peterson model, a total error of 0.9% is determined.

– B-physics

– B-meson mixing: The uncertainty due to mixing in the neutral B sector has been studied by varying the effective mixing parameter (see equation 13) χ_{eff} within its errors. An error of 0.8% is found.

– Branching ratios: The dependence on the branching ratios $b \to \ell$ and $b \to c \to \ell$ has been investigated by varying them within their experimental errors. Mean values and errors used are given in Table 4. An error of 0.8% is found. A breakdown of the error into the different channels contributing is given in Table 6.

– Particle identification

– Electron identification: The efficiency to identify electrons is calculated in the Monte Carlo. The two variables which mainly determine the performance of the neural network are the specific energy loss, $\mathrm{d}E/\mathrm{d}x$, together with its error, and the ratio E/p. Both variables are compared between Monte Carlo and data using different samples of identified particles. The $\mathrm{d}E/\mathrm{d}x$ measurements are calibrated in data using samples of inclusive pions at low momenta and electrons from Bhabha events at 45 GeV/c. The quality of the calibration is checked with a number of control samples, mostly pions from $\mathrm{K_S}$ decays and electrons from photon conversions. The deviation between the mean $\mathrm{d}E/\mathrm{d}x$ measured for these samples in the data, and the mean $\mathrm{d}E/\mathrm{d}x$ in the Monte Carlo, is below 5%. Similarly, the resolution of $\mathrm{d}E/\mathrm{d}x$ is studied in these samples, and is found to be described in the Monte Carlo to better than 8%. The total error from these two effects is found by varying both simultaneously, and is ±2.5% Note that for this analysis, no explicit knowledge of the hadronic background in the sample of lepton candidates is needed, since it is subtracted using the wrong sign sample.
A similar study has been performed for the next most significant input variable, E/p. The E/p resolution in the Monte Carlo is about 10% worse than in the data. The Monte Carlo has been reweighted to the data, and the full difference is used as an estimate of the error, resulting in a variation of the efficiency of ±2.7%.
No significant contributions to the error are found from the other input variables of the network. The error related to them is estimated from the statistical precision of these tests, which is less than 1% of the efficiency. In total, an error of ±4% is assigned to this source.

– Muon identification: The systematic error of the muon identification efficiency is evaluated using a method similar to that described in [15]. The muon detection efficiency is compared between data and Monte Carlo using various control samples, namely $\mathrm{Z^0} \to \mu^+\mu^-$ events, and muons reconstructed in jets. Without using $\mathrm{d}E/\mathrm{d}x$ information, an error of ±2% is found. The influence of the $\mathrm{d}E/\mathrm{d}x$ selection cut on the muon ID is studied in the same way as described for electrons. The mean $\mathrm{d}E/\mathrm{d}x$ for muons in $\mathrm{Z^0} \to \mu^+\mu^-$ events is observed to be shifted by approximately 15% of the resolution in $\mathrm{d}E/\mathrm{d}x$ with respect to the theoretically expected value. A very similar shift is observed in the Monte Carlo, both for muon pairs and for muons identified inclusively in jets. An error of 5% is used.
The $\mathrm{d}E/\mathrm{d}x$ resolution is studied in the data, and is found to be modeled by the Monte Carlo to better than 5%. The final error assigned to the efficiency of muon identification is ±3.0%.

– Internal sources

– Flavour separation: The errors of the flavour composition on the $\mathrm{D^{*+}}$ sample estimated in [13] are used to calculate the corresponding error of the semileptonic branching fractions. A breakdown of the total error into sources correlated and uncorrelated with the reconstruction of leptons in the $\mathrm{D^{*+}}$ sample is given in Table 2, and is taken into account in calculating the final error. The uncorrelated error is 2.8%; the total correlated error is 0.9%.

– Background charge asymmetry: The correction applied to the background-subtracted sample of $\mathrm{D^{*+}}\ell^-$ events is calculated based on the measured fraction of events contributing, and on the charge asymmetry, which comes from Monte Carlo simulation. For the former, the statistical error of the measurement is used as a systematic uncertainty, translating into an error of 1.1%. The Monte Carlo prediction of the charge asymmetry is conservatively varied by ±50% of its value. The final error from this is 2.5%.

– Background estimation: The background in the $\mathrm{D^{*+}}\ell^-$ sample is estimated from the wrong sign sample. The number of combinatorial background events, corrected for mixing and for the effects of the background charge asymmetry, is compared with the expected number of combinatorial background events in the Monte Carlo simulation. Within the statistical precision of this test good agreement is found. The statistical error of this test is used as a systematic uncertainty, resulting in an error of 1.8%. The influence of the p_t cut on the background is studied by comparing the shapes of the background between data and Monte Carlo. The data spectrum is reweighted to the Monte Carlo one, and the number of background events is recalculated. The resulting difference is used as a systematic error of 0.3%. The final error assigned is 1.8%.

– Detector modelling: The influence of the detector resolution on the tagging variables is studied in Monte Carlo simulations by varying the resolutions in the central tracking detectors by ±10% relative to the values that optimally describe the data. The analysis is repeated and the efficiencies are recalculated. The error is 1.1%.
The calculation of the efficiencies relies on the correct modelling of the detector acceptances, in particular in $\cos\theta$. This has been tested by reweighting the $\cos\theta$ distribution of $\mathrm{D^{*+}}$ candidates as found in the Monte Carlo simulation to that reconstructed from data, and repeating the analysis. This changes the result by 0.3%, which is used as a systematic error. The total the error due to detector modelling is 1.2%.

– Gluon splitting: Gluon splitting into a pair of heavy quarks can produce $\mathrm{D^{*+}}$ mesons which might contribute to the sample of selected events. This contribution is found to be (1.1 ± 0.4)%. It is based on the OPAL measurement of gluon splitting [18] and Monte Carlo

Table 6. List of systematic errors contributing to $B(c \to e)$, $B(c \to \mu)$ and $B(c \to \ell)$. A detailed explanation of the different errors can be found in the text

Source	$B(c \to e)$	$B(c \to \mu)$	$B(c \to \ell)$
Modelling			
$c \to \ell$ model	$^{+0.0057}_{-0.0034}$	$^{+0.0050}_{-0.0030}$	$^{+0.0053}_{-0.0031}$
$b \to \ell$ model	0.0001	0.0001	0.0001
$b \to c \to \ell$ model	0.0002	0.0002	0.0002
Fragmentation modelling	0.0010	0.0008	0.0009
Total modelling	$^{+0.0058}_{-0.0035}$	$^{+0.0051}_{-0.0032}$	$^{+0.0054}_{-0.0032}$
B physics			
B-meson mixing	0.0009	0.0008	0.0008
$B(b \to \ell)$	0.0003	0.0002	0.0003
$B(b \to c \to \ell)$	0.0007	0.0006	0.0006
$B(b \to \bar{c} \to \ell)$	0.0005	0.0004	0.0005
$B(b \to \tau \to \ell)$	0.0001	0.0001	0.0001
$B(b \to J/\Psi \to \ell^+\ell^-)$	< 0.0001	< 0.0001	< 0.0001
Total B physics	0.0013	0.0011	0.0012
Particle ID			
Electron identification	0.0041	-	0.0017
Muon identification	-	0.0027	0.0015
Internal sources			
Flavour separation (uncorr.)	0.0028	0.0024	0.0026
Background charge asymmetry	0.0026	0.0023	0.0024
Background estimator	0.0019	0.0016	0.0017
Detector modelling	0.0012	0.0011	0.0011
Gluon splitting	0.0005	0.0004	0.0004
Monte Carlo statistics	0.0024	0.0016	0.0015
Total error	$^{+0.0088}_{-0.0075}$	$^{+0.0072}_{-0.0060}$	$^{+0.0074}_{-0.0060}$

simulation to determine the selection efficiency. The total number of D^{*+} mesons is corrected for this effect. The uncertainty of this number is used as a systematic error of 0.4%. Similarly, leptons can be produced in gluon splitting events. The contribution to the sample is found to be (0.2 ± 0.1)%, which results in an error of 0.1%. According to these studies the total systematic uncertainty is 0.4%.

– Monte Carlo statistics

– Monte Carlo statistics: The efficiencies to identify a lepton in the D^{*+} sample are calculated from the Monte Carlo with limited statistical precision. The error from this source amounts to 1.5%.

A complete list of systematic errors is presented in Table 6 for $B(c \to e)$, $B(c \to \mu)$, and $B(c \to \ell)$. Except for the error from Monte Carlo statistics and the lepton identification errors, all errors from a given source are assumed to be fully correlated between the electron and the muon results.

To check the stability of the results, the analysis is repeated with different selection cuts for the leptons. Consistent results are found if the momentum cut is raised from 2 GeV/c to 3 GeV/c both for electrons and muons, if the transverse momentum cut is removed, if the muon selection is repeated using muons in the central part of the detector only, and if the muon selection is done without using the $\mathrm{d}E/\mathrm{d}x$ selection cut.

8 Conclusions

A measurement of the inclusive charm hadron semileptonic branching fractions in $Z^0 \to c\bar{c}$ events, $B(c \to e)$ and $B(c \to \mu)$, has been presented. The identification of $Z^0 \to c\bar{c}$ events is based on the reconstruction of D^{*+} mesons. The semileptonic branching ratios are measured by reconstructing leptons in the charm-tagged sample and are found to be

$$B(c \to e) = 0.103 \pm 0.009^{+0.009}_{-0.008} \text{ and}$$
$$B(c \to \mu) = 0.090 \pm 0.007^{+0.007}_{-0.006},$$

where the first error is in each case statistical and the second systematic. Combining the two measurements while taking correlations into account, gives

$$B(c \to \ell) = 0.095 \pm 0.006^{+0.007}_{-0.006}.$$

This result agrees well and is competitive with the most recent published measurement at lower energies of $B(c \to \ell) = 0.095 \pm 0.009$ [3].

Acknowledgements. We particularly wish to thank the SL Division for the efficient operation of the LEP accelerator at all energies and for their continuing close cooperation with our experimental group. We thank our colleagues from CEA, DAPNIA/SPP, CE-Saclay for their efforts over the years on the time-of-flight and trigger systems which we continue to use. In addition to the support staff at our own institutions we are pleased to acknowledge the Department of Energy, USA, National Science Foundation, USA, Particle Physics and Astronomy Research Council, UK, Natural Sciences and Engineering Research Council, Canada, Israel Science Foundation, administered by the Israel Academy of Science and Humanities, Minerva Gesellschaft, Benoziyo Center for High Energy Physics, Japanese Ministry of Education, Science and Culture (the Monbusho) and a grant under the Monbusho International Science Research Program, Japanese Society for the Promotion of Science (JSPS), German Israeli Bi-national Science Foundation (GIF), Bundesministerium für Bildung, Wissenschaft, Forschung und Technologie, Germany, National Research Council of Canada, Research Corporation, USA, Hungarian Foundation for Scientific Research, OTKA T-016660, T023793 and OTKA F-023259.

References

1. Particle Data Group, C. Caso et al., *Review of Particle Properties*, Eur. Phys. J. C **3** (1998) 1.

2. K. Mönig, *Status of Electroweak Tests with Heavy Quarks*, CERN-EP/98-78, submitted to Reports on Progress in Physics.
3. ARGUS Collaboration, H. Albrecht et al., Phys. Lett. B **278** (1992) 202; ARGUS Collaboration, H. Albrecht et al., Phys Lett. B **374** (1996) 249.
4. MARK2 Collaboration, R. A. Ong et al., Phys. Rev. Vol. 60 Number **15** (1988) 2587; JADE Collaboration, W. Bartel et al., Z. Phys. C **33** (1987) 339; DELCO Collaboration, T. Pal et al., Phys. Rev. D Vol. 33 Number **9** (1986) 2708.
5. OPAL Collaboration, K. Ahmet et al., Nucl. Instr. Meth. A **305** (1991) 275; P. P. Allport et al., Nucl. Instr. Meth. A **324** (1993) 34; P. P. Allport et al., Nucl. Instr. Meth. A **346** (1994) 476; O. Biebel et al., Nucl. Instr. Meth. A **323** (1992) 169; M. Hauschild et al., Nucl. Instr. Meth. A **314** (1992) 74.
6. OPAL Collaboration, R. Akers et al., Z. Phys. C **65** (1995) 17.
7. T. Sjöstrand, Comp. Phys. Comm. **82** (1994) 74.
8. OPAL Collaboration, G. Alexander et al., Z. Phys. C **69** (1996) 543.
9. C. Peterson et al., Phys. Rev. D **27** (1983) 105.
10. The LEP Collaborations, ALEPH, DELPHI, L3 and OPAL, Nucl. Instr. Meth. A **378** (1996) 101-115; updated averages are given in *'Presentation of LEP Electroweak Heavy Flavour Results for Summer 1996 Conferences'*, LEPHF 96-01 (see `http://www.cern.ch/LEPEWWG/heavy/`).
11. J. Allison et al., Nucl. Instr. Meth. A **317** (1991) 47.
12. JADE Collaboration, W. Bartel et al., Z. Phys. C **33** (1986) 23; JADE Collaboration, S. Bethke et al., Phys. Lett. B **213** (1988) 235.
13. OPAL Collaboration, K. Ackerstaff et al., Eur. Phys. J. C **1** (1998) 439.
14. OPAL Collaboration, G. Alexander et al., Z. Phys. C **70** (1996) 357.
15. OPAL Collaboration, R. Akers et al., Z. Phys. C **60** (1993) 199.
16. OPAL Collaboration, R. Akers et al., Z. Phys. C **60** (1993) 601.
17. OPAL Collaboration, G. Alexander et al., Z. Phys. C **73** (1997) 379.
18. OPAL Collaboration, R. Akers et al., Phys. Lett. B **353** (1995) 595.
19. OPAL Collaboration, P. D. Acton et al., Z. Phys. C **72** (1996) 377.
20. OPAL Collaboration, R. Akers et al., Z. Phys. C **67** (1995) 27.
21. G. Altarelli, Nucl. Phys. B **208** (1982) 365.
22. N. Isgur et al., Phys. Rev. D **39** (1989) 799.
23. P. Collins and T. Spiller, J. Phys. **G 11** (1985) 1289.
24. V. G. Kartvelishvili, A. K. Likhoded and V. A. Petrov, Phys. Lett. B **78** (1978) 615.